CHEMICAL ENGINEERING TRANSACTIONS

VOL. 86, 2021

A publication of AIDIC
The Italian Association of Chemical Engineering
Online at www.cetjournal.it

Guest Editors: Sauro Pierucci, Jiří Jaromír Klemeš

**ISBN** 978-88-95608-84-6; **ISSN** 2283-9216

# Optimal Vulcanization of Unbonded Fiber Reinforced Elastomeric Isolator Devices

Gaetano Pianese[a], Gabriele Milani[a,*], Renato Cerchiaro[b], Federico Milani[c]

[a]Politecnico di Milano, Piazza Leonardo da Vinci 32, 20133 Milano, Italy
[b]Dergom S.R.L, Via dei Castagni, 3/5, 23846 Garbagnate Monastero (LC), Italy
[c]Chem. Co Consultant, Via J.F.Kennedy 2, 45030 Occhiobello (RO), Italy
gabriele.milani@polimi.it

Elastomeric seismic isolation is a technique diffused in civil engineering to protect existing and new structures against earthquakes. It consists in introducing between the superstructure and the foundation several devices (called seismic isolators) having the property to carry vertical loads maintaining at the same time the shear modulus small, increasing considerably the natural period of the structure, where the spectral acceleration drops down (Habieb et al., 2020 and 2019a, 2019b, 2019c, 2019d, 2018). This study investigates the possibility of using recycled rubber in the form of reactivated EPDM (made by 2/3 of regenerated rubber and 1/3 of virgin rubber) for the production of low cost rubber isolators (Habieb et al., 2020). A Fiber Reinforced Elastomeric Isolator FREI prototype constituted by five EPDM pads and four GFRP laminas interposed between contiguous pads is cured in the lab at 130°C and the level of vulcanization is experimentally provided measuring Shore A hardness on several points. A 3D numerical model based on both finite differences and FEM is proposed to predict the degree of vulcanization of the FREI numerically. It is found that the crosslinking density obtained is suboptimal (but still acceptable for an engineering point of view) and that it is required to increase the vulcanization temperature to obtain a full and homogeneous curing.

## 1. Introduction

Innovative retrofitting strategies illustrated in Section 2 can be used to mitigate the effect of earthquakes, with the aim of decreasing the seismic demand on the structure or increasing its energy dissipation capacity. One of the most innovative devices is the Unbonded Fiber Reinforced Elastomeric Isolator system UFREI. UFREI is made of alternate layers of fiber and rubber and UFREIs are interposed between the ground and the foundation, with the particularity that no bonding or fastening is provided between the bearing and top-bottom supports. In this study the best curing conditions to vulcanize homogeneously a seismic isolator constituted by five EPDM (made by 2/3 of regenerated rubber and 1/3 of virgin rubber) pads and four GFRP laminas are investigated. A full 3D numerical model based on standard Finite Differences (validated with FEM), coupled with a crosslinking Arrhenius law, is used. The prototype is cured here first at 130°C for 40 minutes, then at 140°C for 40 minutes and finally at 150°C for 40 minutes. It is found that the crosslinking density obtained with the latter vulcanization is optimal, exhibiting a full and homogeneous curing.

## 2. Experimentation carried out

The experimental performance of four rubber batches with regenerated EPDM is evaluated in an experimental campaign proposed in Habieb et al. (2020). Vistalon 3666 and Dutral 2038, two commercial virgin rubbers, are blended with two regenerated EPDMs (Type A, less performant and type B, exhibiting a better quality) to obtain blends with hardness 30±5 ShA and 60±5 ShA. As discussed in Habieb et al. (2020), after several experimentations, Batch 4B showed the best performance and it is here used to cure the FREI prototype studied numerically.

*Table 1: Four different batches experimentally tested to select the best blend with re-generated rubber to produce the elastomeric isolator prototype*

| **Batch 1A** | **Batch 2B** | **Batch 3A** | **Batch 4B** |
|---|---|---|---|
| Vistalon 3666 | Vistalon 3666 | Dutral 4038 | Dutral 4038 |
| Regenerated EPDM (Type A) | Regenerated EPDM (Type B) | Regenerated EPDM (Type A) | Regenerated EPDM (Type B) |
| 30 ± 5 ShA | 30 ± 5 ShA | 60 ± 5 ShA | 60 ± 5 ShA |

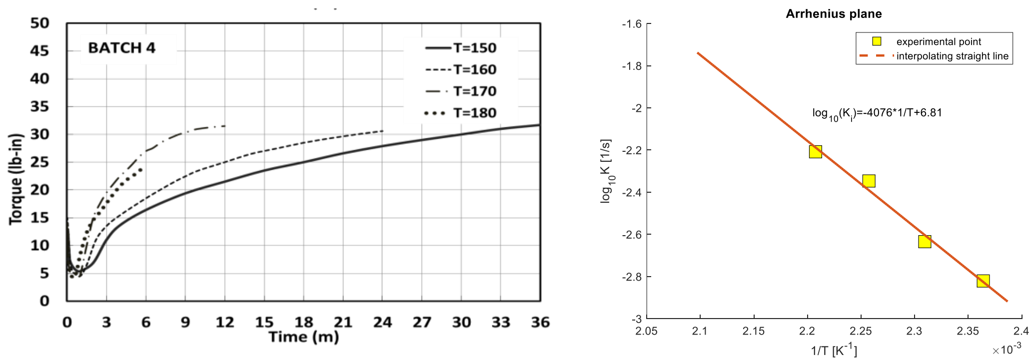


a b

*Figure 1: a) Rheometer curves obtained for batch 4B. b) experimental determination by linear best fitting of the reaction kinetic constant for the rubber blend.*

## 3. Rheometer curves and determination of the kinetic behavior

According to the experimental rheometer curves obtained at 4 different temperatures (from 150°C to 180°C), it is found that a blend between virgin and regenerated rubber follows a classic crosslinking law ruled by the following equation (P and P* are respectively the uncured and cured polymer, whereas K(T) is the kinetic constant, variable with the temperature T ruling the reaction):

$$P \xrightarrow{K(T)} P^* \tag{1}$$

Which allows to find the degree of vulcanization against the curing time *t*:

$$\alpha_R = 1 - e^{-K(T)t} \tag{2}$$

In the previous equation K(T) is ruled by the following absolute temperature dependent logarithmic law:

$$log_{10}K(T) = log_{10}K_{max} - \frac{E_a}{R_g}\frac{1}{T} \tag{3}$$

Where $K_{max}$ is the kinetic constant at an infinite temperature T, $E_a$ is the activation energy and $R_g$ the gas constant. After normalization of the rheometer curves obtained experimentally (Figure 1a) it was possible to evaluate parameters $log_{10}K_{max}$ and $-\frac{E_a}{R_g}$ by linear interpolation of experimental data (Figure 1b) and predict $\alpha_R$ in each point of the isolator once that the temperature profile during curing is known, for instance solving a heat transmission law using finite differences. In Figure 1, only results for Batch 4B are reported, because it was found that such batch shows the best performances. Much more complex models are under development, in agreement with Milani & Milani (2018a, 2018b, 2017) and Milani et al. (2015).

## 4. Finite differences method

When finite differences are used to evaluate the temperature profile inside an item, the following forward scheme can be used, once that the item is discretized into pixels of dimensions $\Delta x$ and $\Delta y$:

$$T_{m,n}^{p+1} = T_{m,n}^{p} + \alpha\frac{\Delta t}{\Delta x^2}\left(T_{m+1,n}^{p} - 2T_{m,n}^{p} + T_{m-1,n}^{p}\right) + \alpha\frac{\Delta t}{\Delta y^2}\left(T_{m,n+1}^{p} - 2T_{m,n}^{p} + T_{m,n-1}^{p}\right) \tag{4}$$

Where $m$ and $n$ indicate the ($m,n$) pixel, $p$ the time, $\Delta t$ the time interval and $\alpha = \frac{K}{\rho c}$, where $K$ is the conductivity, $c$ the heat capacity and $\rho$ the density. According to trivial thermodynamics constrains, the time increment must non exceed the following value:

$$\Delta t < \frac{\Delta x^2 \Delta y^2}{2\alpha(\Delta x^2 + \Delta y^2)} \tag{5}$$

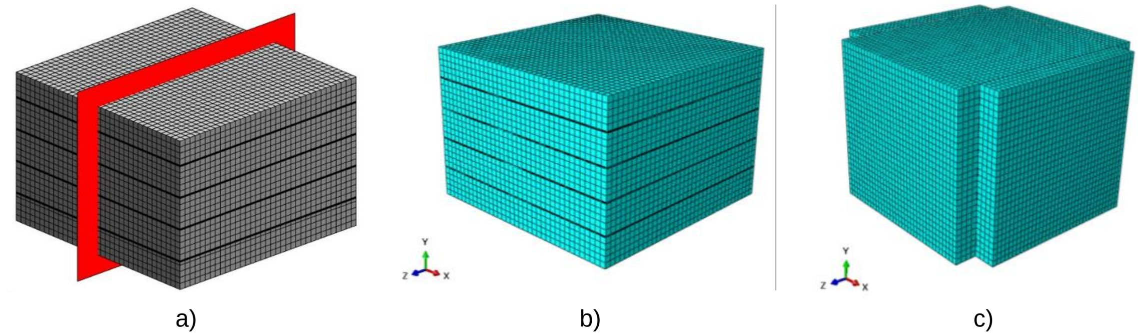


*Figure 2: Discretization of the isolator into 3D finite differences (a), into 3D finite elements (b) and into 3D finite elements with steel mould (c).*

Voxels used here use the same concept, but following a tri-dimensional discretization of the isolator as shown in Figure 2.

## 5. Numerical results

Numerical results obtained vulcanizing the isolator at different temperatures (130°C, 140°C and 150°C) for 40 minutes are provided in Figures 2, 3, 4 and 5. In particular Figure 2 shows the discretization of the isolator into 3D finite differences (a), into 3D finite elements (b) and into 3D finite elements where the steel mold is meshed with an equivalent thickness of 10 mm and a heat conductivity of 0,06 W/mm*K with the aim of reproducing more realistically the experimental conditions observed in the vulcanization oven. The temperature profile and the crosslinking degree are numerically evaluated in the central section (red plane). Figures 3,4 and 5 show comparisons between the vulcanization levels obtained with finite differences and FEM for a point in the middle of the central cross section (top subfigures) and near the corner (bottom subfigures). In particular, on the left they show the position of the point considered and the temperature profile obtained numerically, whereas on the right they depict the numerically obtained crosslinking degree.

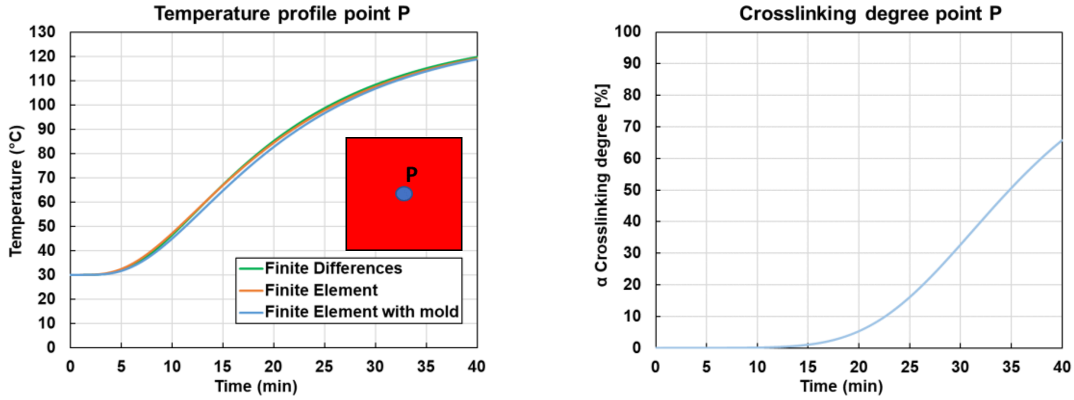

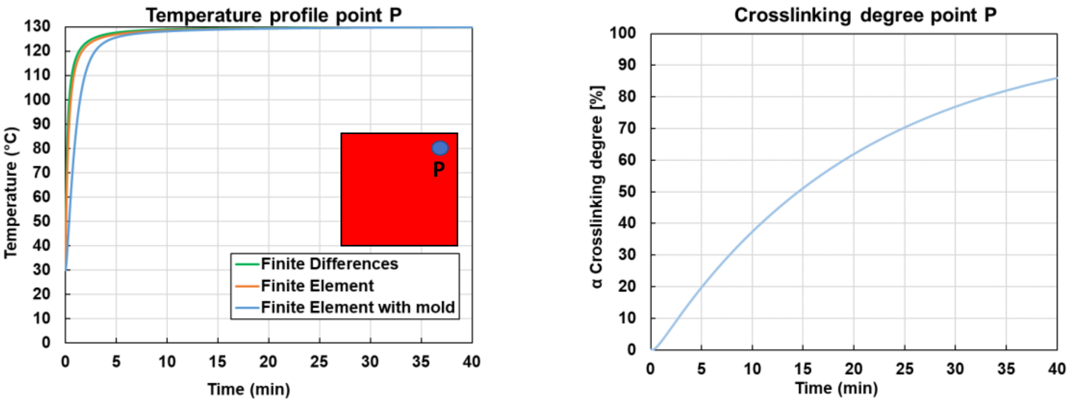


a) b)

*Figure 3: Comparison between the vulcanization level obtained numerically with Finite Differences and FEM (with and without mold) for a point in the middle of the central cross section and near the corner (T=130°C): a) temperature profile. b) crosslinking degree.*

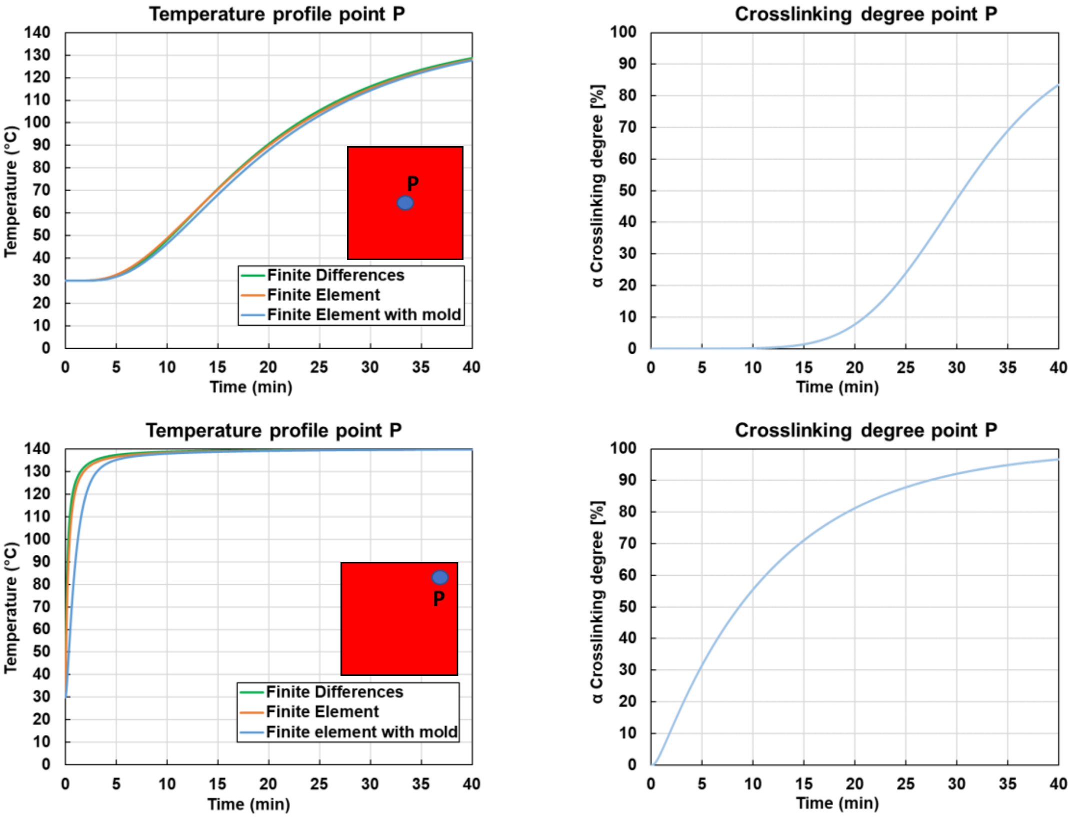


a) b)

*Figure 4: Comparison between the vulcanization level obtained numerically with Finite Differences and FEM (with and without mold) for a point in the middle of the central cross section and near the corner (T=140°C): a) temperature profile. b) crosslinking degree.*

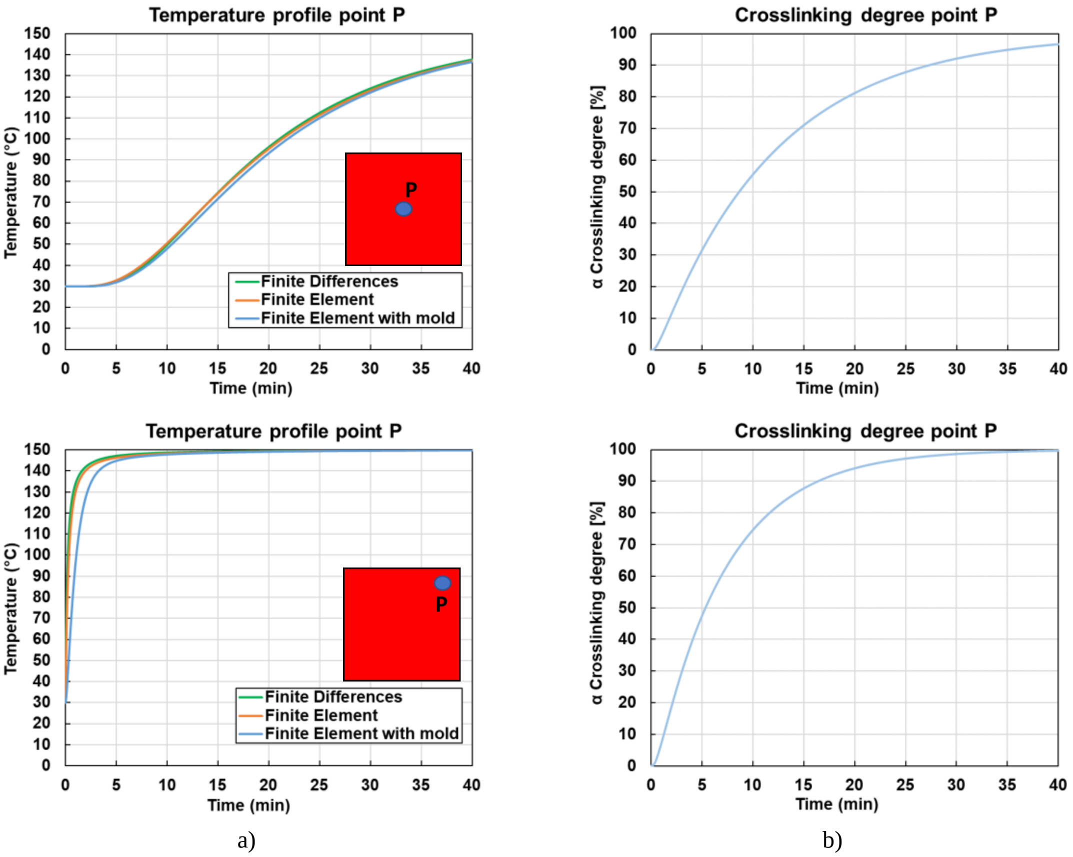


*Figure 5: Comparison between the vulcanization level obtained numerically with Finite Differences and FEM (with and without mold) for a point in the middle of the central cross section and near the corner (T=150°C): a) temperature profile. b) crosslinking degree*.

In order to investigate the distribution of crosslinking degree obtained from the various vulcanizations in all the device, the study was extended also for central and corner points of different planes of the device, parallel to the first one considered (Figure 6). The results are shown in Figure 7.

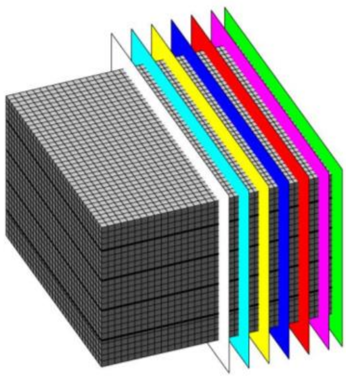

*Figure 6: planes considered to investigate the crosslinking density*

## 6. Conclusions

The results show that near the corner, the vulcanization degree is quite high whereas in the center of the isolator is much lower for a vulcanization temperature of 130°C and less for 140°C. The same behavior can be found for the other planes. So, the crosslinking density obtained at 130°C and at 140°C is suboptimal, but still acceptable from an engineering point of view, whilst at 150°C a full and homogeneous curing is obtained.

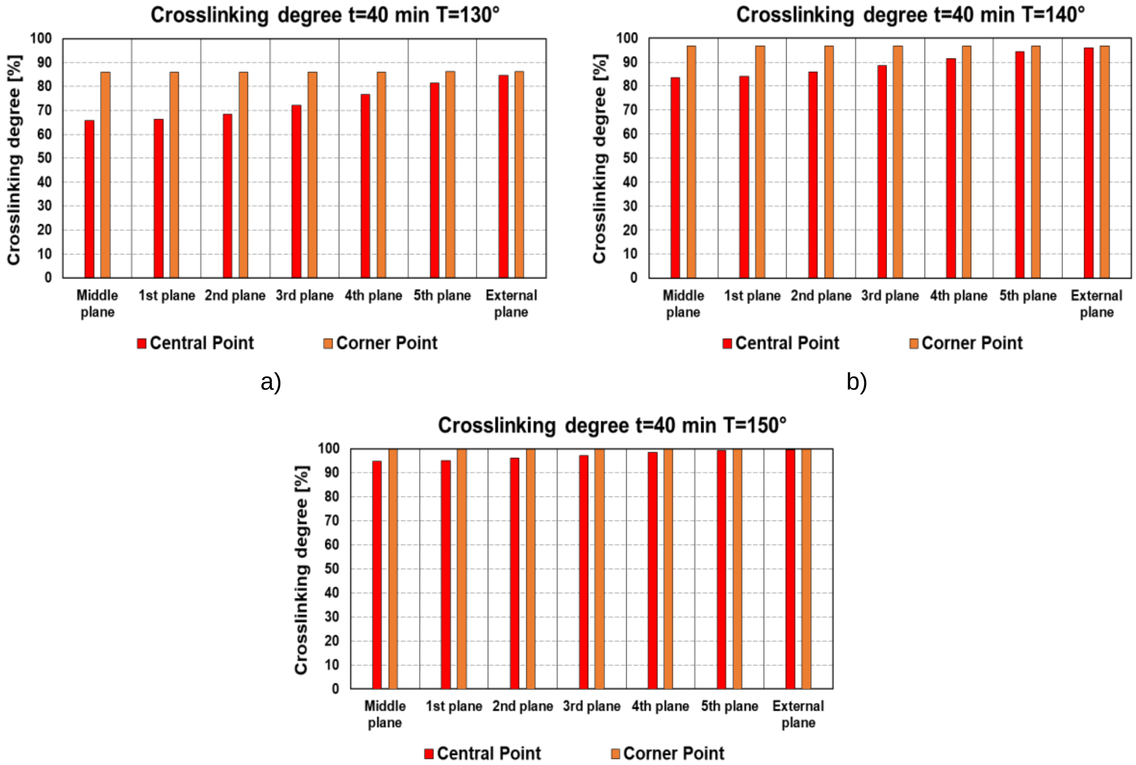


a) b) c)

*Figure 7: Crosslinking degree of central and corner points for different planes: T=130°C (a), T=140°C (b) and T=150°C (c).*

## References


Habieb, A.B., Milani F., Milani, G., Cerchiaro, R., 2020. Rubber compounds made of reactivated EPDM for fiber-reinforced elastomeric isolators: an experimental study. Iranian Polymer Journal (English Edition); 29(11), 1031-1043. DOI: 10.1007/s13726-020-00859-9.

Habieb A.B., Milani G., Quaglini V., Milani F., 2019a. Experimentation and numerical modelling of recycled rubber pads for seismic isolation under accelerated ageing. AIP Conference Proceedings; 2116, # 420006.

Habieb A.B., Valente M., Milani G., 2019b. Hybrid seismic base isolation of a historical masonry church using unbonded fiber reinforced elastomeric isolators and shape memory alloy wires. Engineering Structures; 196, #109281.

Habieb, A.B., Valente, M., Milani, G., 2019c. Effectiveness of different base isolation systems for seismic protection: Numerical insights into an existing masonry bell tower. Soil Dynamics and Earthquake Engineering; 125, # 105752.

Habieb A.B., Valente M., Milani G., 2019d. Base seismic isolation of a historical masonry church using fiber reinforced elastomeric isolators. Soil Dynamics and Earthquake Engineering; 120, 127-145.

Habieb A.B., Milani G., Tavio T., 2018. Two-step advanced numerical approach for the design of low-cost unbonded fiber reinforced elastomeric seismic isolation systems in new masonry buildings. Engineering Failure Analysis; 90, 380-396.

Milani F., Milani G., 2018a. Rubber blends: kinetic numerical model by rheometer experimental characterization. Journal of Mathematical Chemistry, 56, 1520–1542.

Milani G., Milani F., 2018b. Optimal vulcanization of tires: Experimentation on idealized NR-PB natural and poly-butadiene rubber blends, phenomenological smoothed numerical kinetic model and FE implementation, Polymer Testing; 72, 63-85.

Milani F., Milani G., 2017. Comprehensive kinetic numerical model for NR and high-cis poly-butadiene rubber blends. Chemical Engineering Transactions; 57, 1495-1500.

Milani G., Hanel T., Milani F., Donetti R., 2015. A closed form solution for the vulcanization prediction of NR cured with sulphur and different accelerators. Journal of Mathematical Chemistry; 53(4), 975-997.